Turk J Phys
27 (2003) , 383 – 393.

Quantum Computing with Electrons on Liquid Helium

İsmail KARAKURT
Dept. of Physics, Case Western Reserve University,
Cleveland, OH 44106, USA

Received 12.09.2003

Abstract

A quantum computer based on electrons floating over liquid helium is described. Each qubit is made of combinations of ground and first excited states of an electron trapped over micro-electrodes just below the helium surface. We describe mechanisms for preparing the initial state of the qubit, operations with the qubits, and a proposed readout. This system is, in principle, capable of $\sim 10^4$ operations in a decoherence time, the time in which the wave function collapses.

Key Words: Quantum computing, Decoherence, Electrons on helium.

1. Introduction

Quantum computing invokes the use of energy levels of a quantum system for bits. It has the potential of being extremely fast and handling large simulations. Many designs for a quantum computer (QC) have been proposed.[1] We give a description of a design based on quantum bits comprised of electrons bound to a helium surface.[1, 2, 3, 4, 5, 6] Each quantum bit (qubit) is made of combinations of ground and first excited states of an electron trapped over micro-electrodes just below the helium surface.

A quantum computer uses two stationary states of a quantum system as counterparts of the classical bits 0 and 1. We identify the ground and first excited states of these electrons with the $|0\rangle$ and $|1\rangle$ analog of classical bits, respectively. Each qubit can be put in any linear superposition of the states $|0\rangle$ and $|1\rangle$,

$$\psi_j = a_j|0\rangle + b_j|1\rangle, \quad |a_j|^2 + |b_j|^2 = 1. \tag{1}$$

Here, $|a_j|^2$ and $|b_j|^2$ are the probabilities of finding the qubit j in the states $|0\rangle$ and $|1\rangle$, respectively. In simple cases $a_j, b_j = 0$, 1 or $2^{-1/2}$.

A quantum computer composed of N qubits has 2^N basis states (combinations of $|0\rangle$s and $|1\rangle$s for each qubit) which in the simplest form are products of the basis vectors of each of the N qubits. The general state of a QC is written as

$$\Psi = \sum_j \alpha_j|x_j\rangle, \quad \sum_j |\alpha_j|^2 = 1, \tag{2}$$

where $|x_j\rangle$ is one of the 2^N basis vectors. An example of a four-qubit system is

$$\Psi = 2^{-1/2}(|1\rangle + |0\rangle)|0\rangle|1\rangle|0\rangle = 2^{-1/2}(|1\rangle|0\rangle|1\rangle|0\rangle + |0\rangle|0\rangle|1\rangle|0\rangle). \tag{3}$$

The state is called an entangled state if the superposition can not be made up of a product of individual states. For a two-qubit system an entangled state can be

$$\Psi = 2^{-1/2}(|11\rangle + |00\rangle). \tag{4}$$

Operations use qubits in a superposition of many possible basis states and can, therefore, be equivalent to performing a large number of computations in parallel. The difficulty in utilizing this advantage arises from the fundamental nature of measurement in quantum processes, namely that measurement of the energy of an individual qubit will necessarily collapse the wave function so that the result can be only either $|0\rangle$ or $|1\rangle$ for each qubit. This requires algorithms that can yield definite answers to computations. We describe mechanisms for preparing the initial state of the qubit, operations with the qubits, and a proposed readout. This system is, in principle, capable of $\sim 10^4$ operations in a decoherence time, the time in which the wave function collapses.

We choose the ground and first excited states associated with the motion of an electron normal to the liquid helium surface for the states $|0\rangle$ and $|1\rangle$, respectively. Electrodes beneath the electrons are used to localize them laterally and to apply a Stark field to each qubit individually. Data is read into the registers by preparing each qubit in an admixture of states $|0\rangle$ and $|1\rangle$. This is accomplished by Stark shifting states sequentially into resonance with microwave radiation for a predetermined length of time. For the operations of gates, interactions between neighboring qubits are controlled by Stark shifting their energy levels into resonance with each other and applying rf pulses of radiation for a specified time. The answer to the calculation is in the final state of the qubits. We propose a mechanism for a simultaneous readout of each qubit. It involves extracting electrons in the weakly bound excited state, $|1\rangle$, with an electric field ramp while leaving electrons in the ground state, $|0\rangle$, above micro electrodes. Then tunneling of the remaining electrons will be probed with a superconducting bolometer placed right above micro electrodes. The mechanisms that cause relaxation, T_1 and T_2 processes, will be discussed.

2. Electrons on Helium

An electron placed at a distance z above a liquid helium surface polarizes the helium atoms in the liquid. This polarization can be described mathematically with an image charge $+e(\epsilon-\epsilon_0)/(\epsilon+\epsilon_0)$ in the liquid at a distance z below the surface. Here, $\epsilon = 1.0568$ and ϵ_0 are the dielectric constants of liquid ^{4}He and the vapor, respectively. The electron is prevented from entering the liquid due to Pauli force. The s-shell of the helium atoms in the liquid is completely filled. The wave function of any extra electron must be orthogonal to those of the core electrons in the liquid, and, as a result, must have p-wave characteristics. This requires energy of ~ 1 eV which prevents the electron from penetrating into the liquid. The binding energy of the electron is small compared to this potential barrier. Therefore, one can assume that this potential barrier is infinite compared to the potential energy due to the image charge and the applied field, and solve the Schrödinger equation for the electron accordingly.

In an externally applied field F, the Hamiltonian H, of the electron is given by

$$H = -\frac{\hbar^2}{2m}(\frac{d}{dz})^2 - \frac{Qe^2}{z+z_0} + eFz. \tag{5}$$

where $Q = (\epsilon-\epsilon_0)/4(\epsilon+\epsilon_0)$ and the surface of the liquid is assumed to be at $z = 0$. The constant $z_0 = 1.04$ Å in the image potential term in H has been introduced to obtain the exact energy spectrum[7] of an electron on liquid helium. The correction is necessary since the surface is not perfect, i.e. the liquid density drops to zero over a width of about 6-7 Å at the surface.

The Schrödinger equation, $H\phi_n = E_n\phi_n$, for the electron is identical to the equation for $rR(r)$ of the zero angular momentum states of the hydrogen atom for $F = 0$ and $z_0 = 0$. The difference here is that the nuclear charge is reduced by a factor of Q $\sim$0.0069. Thus one obtains hydrogen-like solutions for the wave functions and energy eigenvalues. The ground and the first excited states are given by

$$\phi_1(z) = \frac{2}{b^{3/2}} z e^{-z/b},$$
$$\phi_2(z) = \frac{1}{(2b)^{3/2}}(2-\frac{z}{b}) z e^{-z/2b}, \tag{6}$$

where $b = 76$ Å is the effective Bohr radius. Numerical solutions for ϕ_1 and ϕ_2 at $F = 40$ V/cm are plotted in Fig. 1. Average distance of an electron from the surface is 11.4 nm and 45.6 nm in the ground and first excited states, respectively.

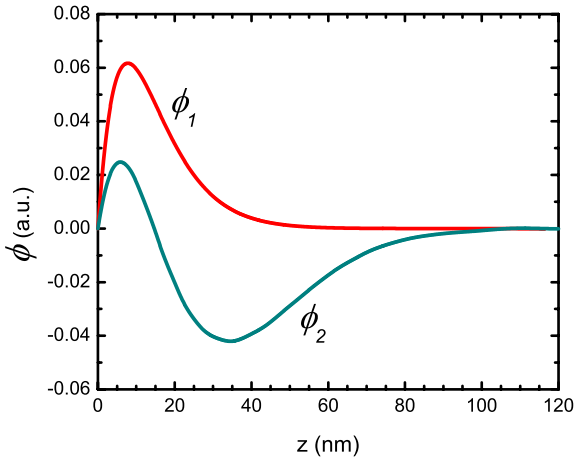

Figure 1. Numerical solutions of the Schrödinger equation for ϕ_1 and ϕ_2 at $F = 40$ V/cm as a function of z.

As in the hydrogen atom, the electron energy is quantized in the direction perpendicular to the surface, and given by

$$E_n = -\frac{R}{n^2}, \quad (n = 1, 2, ...), \quad R = \frac{\hbar^2}{2mb^2} = 8K, \quad b = \frac{\hbar^2}{me^2Q}. \tag{7}$$

At temperatures below ~ 2 K all electrons will be in the ground state. The transition frequency between the ground and the first excited states is ~ 126 GHz. A finite electric field F applied perpendicular to the surface Stark-shifts the energy levels. The confining potentials are shown in Fig. 2 for the cases $F = 0$ and $F > 0$. The Fermi temperature $T_f = \pi\hbar^2 n/mk_B$ is ≤ 2.8 mK for electron densities $n \leq 10^8$ cm^{-2} which will

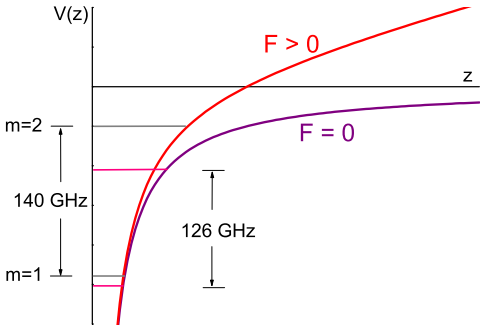

Figure 2. Schematic of the confining potentials in the direction perpendicular to the liquid surface for $F = 0$ and $F > 0$. The transition frequency between the energy levels is a function of the aplied field F.

be used in this project. Therefore electrons are classical even at the low experimental temperature of ~ 10 mK. Without any trapping potentials, electrons are free to move parallel to the surface.

Electrons scatter from helium vapor atoms at high temperatures above 0.7 K. Below 0.7 K the vapor pressure is extremely small and scattering from vapor atoms can be neglected. At 10 mK the coupling of electrons to the external world is via ripplon scattering.

The advantages of using electrons on helium for quantum computing are the simultaneous readout and the scalability. This system has also been studied extensively both theoretically and experimentally. Electrons

have extremely long relaxation time (highest mobility known in a condensed matter system),

$$\tau_0 \sim 10^{-7} \text{ s}, \quad \mu \sim 10^4 - 10^5 \text{ m}^2/\text{Vs}. \tag{8}$$

Inter-electron distance is comparatively large, ~ 1 μm. This makes it easier to construct the micro-structures which will be used to control qubits.

3. Design of the computer

We identify the ground state (n=1) as $|0\rangle$, and the first excited state (n=2) as $|1\rangle$. In order to address and control the qubits each electron is localized laterally over micro electrodes (posts) which would be submerged into the liquid. The distance between micro electrodes is 1 μm while the electrons are separated from the posts by a 0.5 μm thick helium film. The lateral confinement of electrons results from the voltages applied to the posts and the potential due to the image charge at the tips of the posts. A schematic of a four-qubit system is shown in Fig. 3. Electrode potentials lead to Stark shift of the energy levels, and quantization of motion parallel to the surface. The relaxation rate of a confined electron can be much less than that

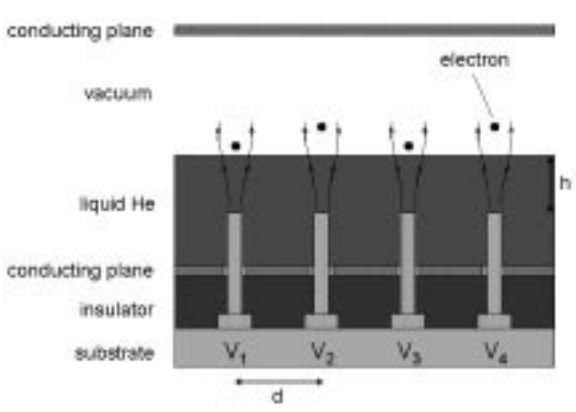

Figure 3. The geometry of a four-qubit system with electrons trapped above micro electrodes. Electric field lines are shown. The drawing is not to scale. The optimal dimensions are d = 1 μm, h = 0.5 μm.

of a free electron. To further slow down the relaxation a magnetic field perpendicular to the surface can be applied.[2] In Fig. 4. we show a schematic of an electron trapped over a microelectrode representing a qubit. In order to obtain a realistic estimate of the electrode potential $U_{\|}$ and the electron energy spectrum,

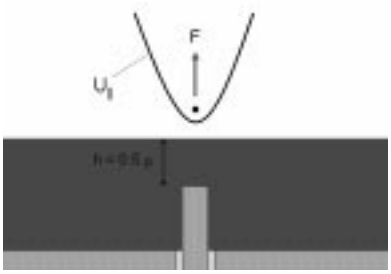

Figure 4. Schematic of the lateral confinement potential $U_{\|}$ and an electron trapped by it. The potential is formed by the electrostatic image in the liquid, the potential from the electrode, potential created by the ground plate and a parallel plate above the electron which is not shown. The figure is not to scale. In reality, $h \gg b$.

Dykman *et al.* [8] used a model in which the micro electrode is approximated as a conducting sphere with a diameter $2r_{el}$ equal to the electrode diameter. For $z \ll h$, $r = (x^2 + y^2)^{1/2} \ll h$, this model gives electron potential energy as

$$U_{\|}(r,z) \cong -\frac{Qe^2}{z} + eFz + \frac{1}{2}m\omega_{\|}^2 r^2$$
$$F = \frac{V_{el}r_{el}}{h^2} + \frac{er_{el}h}{(h^2 - r_{el}^2)^{1/2}}$$
$$\omega_{\|} = (\frac{eF}{mh})^{1/2}. \tag{9}$$

where V_{el} is the electrode potential and $\omega_{\|}$ is the frequency of in-plane oscillations. In-plane electron potential is parabolic near the minimum and leads to harmonic oscillations with the frequency $\omega_{\|}$. Full electron energy spectrum is shown in Fig. 5. Each energy level E_n gives rise to a set of harmonic oscillations parallel to the helium surface with a spacing $\hbar\omega_{\|}$. Both $|0\rangle$ and $|1\rangle$ correspond to the ground state of in-plane vibrations. For typical $F \sim 300$ V/cm and $h \sim 0.5$ μm, one obtains $\omega_{\|}/2\pi \sim 20$ GHz ~ 1 K. Even though the spacing $\hbar\omega_{\|}$ between vibrational levels is less than the energy gap $\Delta E = E_2 - E_1 \sim 8 - 10$ K, with such large $\omega_{\|}$ one can avoid resonance between E_2 and an excited vibrational level of the state $|0\rangle$.

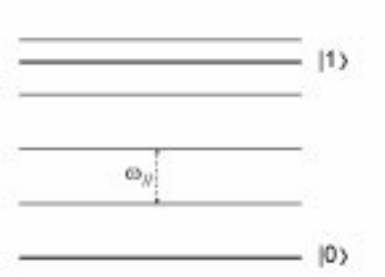

Figure 5. Energy spectrum for a single qubit.

Energy spectrum for a single qubit differs from that of a many-qubit system. Electron-electron interactions come into play in the case of many-qubits. Interaction leads to coupling of in-plane vibrations of different electrons. In a many-electron system the vibrational energy spectrum becomes nearly continuous as a result of a plasmon band associated with each level.[8] In order to avoid quasi-elastic scattering by

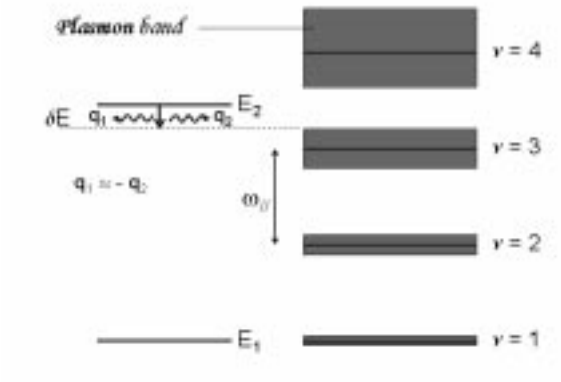

Figure 6. Energy spectrum for multi-qubits. $\nu\Delta_{\|}$ is the width of the plasmon band on the ν^{th} vibrational level.

ripplons, the electron energy spectrum has to be discrete, i.e. broadened vibrational levels should be well separated from each other up to energies $E_2 - E_1$. This requires

$$\Delta_{\parallel} \ll \frac{(\hbar\omega_{\parallel})^2}{E_2 - E_1} = \frac{\hbar\omega_{\parallel}}{\nu}, \tag{10}$$

where, ν is the number of vibrational levels between the levels E_2 and E_1.

For multi-qubit system one must choose suitable values for h, d_{ij}, V_i to optimize the performance of the quantum computer. The objective is to have a high working frequency Ω_{QC} and a low relaxation rate Γ. The frequency Ω_{QC} is determined by the rate of single qubit operations and by the strength of the interaction between neighboring qubits.

The value of $\Delta_{\parallel}$ depends on the geometry. If the electrons form a Wigner crystal with the same lattice constant as the micro electrodes, then the vibrational frequencies $\omega_{\parallel}$ of the pinned crystal are

$$\omega_{\parallel} \sim (\omega_k^2 + \omega_{\parallel})^{1/2} \tag{11}$$

where, ω_k is the phonon frequency of the electron crystal in the absence of electrode potential.[8] If $\omega_k \ll \omega_{\parallel}$, then the phonon bandwidth $\Delta_{\parallel}$ is small compared to $\omega_{\parallel}$, and

$$\Delta_{\parallel} = \frac{max\omega_k^2}{\omega_{\parallel}} \sim \frac{\omega_p^2}{\omega_{\parallel}}, \;\; \omega_p = \frac{2\pi e^2 n^{3/2}}{m}, \tag{12}$$

where, ω_p is the characteristic zone boundary frequency of the Wigner crystal. Therefore, quasi-elastic scattering will be eliminated[8] for a pinned Wigner crystal if

$$\Delta_{\parallel} = \frac{(\hbar\omega_{\parallel})^2}{E_2 - E_1} \;\; \Rightarrow \omega_p^2 \ll \frac{\hbar^2\omega_{\parallel}^3}{E_2 - E_1}. \tag{13}$$

This imposes an upper limit on the nearest neighbor spacing d, because

$$\omega_p \propto \frac{1}{d^{3/2}}. \tag{14}$$

For a square lattice with $d = 1$ μm, one obtains $\omega_p/2\pi = 6.3$ GHz. It has been found theoretically[8] that, in the case of multi-qubits, the frequency $\omega_{\parallel}$ remains close to the single-qubit value for $h/d \leq 0.5$. Therefore, the optimal dimensions for this system would be such that $h = 0.5$ μm and $d = 1$ μm.

4. Qubit-qubit interactions

Wave functions of electrons do not overlap and the important part of the interaction between qubits is dipolar. The dipol-dipol interaction energy V_{ij} , between qubits i and j is given by

$$V_{ij} \sim \frac{e^2(z_i - z_j)^2}{d_{ij}^3}. \tag{15}$$

where, z_i and z_j are the separation of the i^{th} and j^{th} qubits from the surface. For a typical dipole moment eb , the interaction energy V_{ij} between the qubits separated by a distance $d_{ij} = 1$ μm is

$$V_{ij} = \frac{e^2b^2}{d_{ij}^3} \sim 2 \times 10^7 \text{ Hz} \;\; \sim 1 \text{ mK}. \tag{16}$$

Dipolar interaction energy is extremely sensitive to the separation d_{ij} and can be controlled by adjusting the inter-electron distance. For inter-electron distances $d \leq 1$ μm, the qubit-qubit interaction limits the clock frequency of the computer Ω_{QC} to $10^7 - 10^8$ Hz.

5. Operations

5.1. Single-qubit operations

The single-qubit operation yields an admixture of states $|0\rangle$ and $|1\rangle$ by Stark shifting the states into resonance with microwave radiation for a predetermined time. The state of the qubit j evolves as

$$\psi_j = \cos(\frac{1}{2}\Omega\tau_j)|0\rangle - i\sin(\frac{1}{2}\Omega\tau_j)|1\rangle \tag{17}$$

where $\Omega = eE_{rf}\langle 0|z|1\rangle/\hbar$ is the Rabi frequency and τ_j is the time the j^{th} qubit is in resonance with the microwave field E_{rf}. For typical $E_{rf} = 1$ V/cm, $\Omega \cong 10^9$ s^{-1}. Thus, the rate of single qubit operations does not limit the clock frequency of the quantum computer.

5.2. Two-qubit operations

Interactions occur when neighboring qubits are brought into resonance for a predetermined amount of time by giving both states an equal Stark shift. As a result of dipolar interaction between the qubits, an exchange (SWAP) occurs in about 10 ns. The SWAP operation would work in the following manner. Suppose we begin with a two-qubit system in the state $|01\rangle$. Each qubit evolves as

$$\psi_j = \cos(\frac{1}{2}\Omega\tau)|0\rangle - i\sin(\frac{1}{2}\Omega\tau)|1\rangle, \tag{18}$$

where Ω is determined by the strength of the interaction energy. The operation is a SWAP if $\Omega\tau = \pi$,

$$U_{\text{Swap}}|01\rangle \rightarrow i|10\rangle. \tag{19}$$

The operation is a SQUARE ROOT of SWAP if $\Omega\tau = \pi/2$,

$$\sqrt{U_{\text{Swap}}}|01\rangle \rightarrow 2^{-1/2}(|01\rangle + |10\rangle). \tag{20}$$

The operator $\sqrt{U_{Swap}}$ leads to entanglement.

Two-qubit CNOT gate is implied by making use of the interaction between qubits. The transition frequency of an electron depends on the position of the neighboring electron. Fig. 7. shows how the transition frequency ν of the target qubit is affected by the control qubit. If the control qubit $|C\rangle = |1\rangle$, then ν is larger than ν_0 by a factor which is determined by the interaction energy. The ν_0 is the transition frequency for a single qubit. For the CNOT gate the microwave frequency for target transition is selected for the case $|C\rangle = |1\rangle$, for example. Then, the transition in the target qubit will occur only if the control qubit $|C\rangle = |1\rangle$.

6. Readout

The wave function of the system collapses when a measurement is made. It would be advantageous to read all qubits simultaneously. This should be done within the time scale set by the plasma frequency $\omega_p \sim 10$ GHz, i.e. before the qubits interact with one another. We present a simultaneous readout scheme which is destructive. An ~ 1 ns ramp of an extracting field is applied to the top electrode. When the field is sufficiently large, electrons in the excited $|1\rangle$ state will tunnel into the vacuum in a short time while electrons in the ground $|0\rangle$ state will not. The tunneling probability depends exponentially on the extracting field in the range where the WKB approximation holds,

$$P(z) \propto \exp[K(z)dz], \;\; K(z) = [\frac{2m[V(z) - E_2]}{\hbar^2}]^{1/2}. \tag{21}$$

The potential with an extracting field is shown in Fig. 8. Nearly all electrons in the excited state tunnel simultaneously as the tunneling probability changes rapidly from a value of $\ll 10^{-9}$ s^{-1} to a probability $\geq 10^{-10}$ s^{-1} during the field sweep. Later $|0\rangle$ states are extracted sequentially with a large field applied for a longer time to each post.[9] Electrons will be detected by a superconducting bolometer placed above the posts. If an electron is detected, the state was $|0\rangle$. If no electron is detected, the state was $|1\rangle$ (See Fig. 9.).

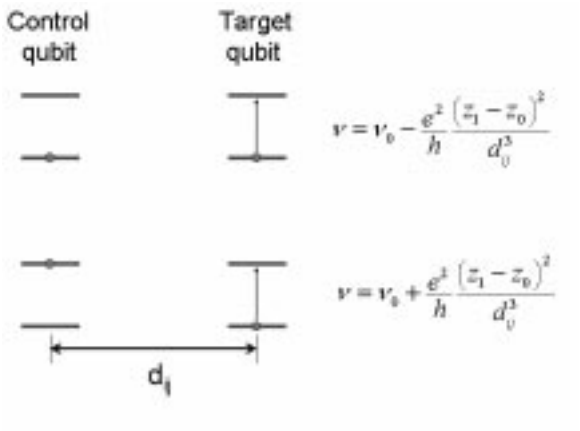

Figure 7. Transition frequency of the target qubit depends on the state of the control qubit. Microwave frequency for target transition can be selected for the cases $|C\rangle = |1\rangle$ or $|C\rangle = |0\rangle$ to oparate the CNOT gate. In the figure, $h = 2\pi\hbar$.

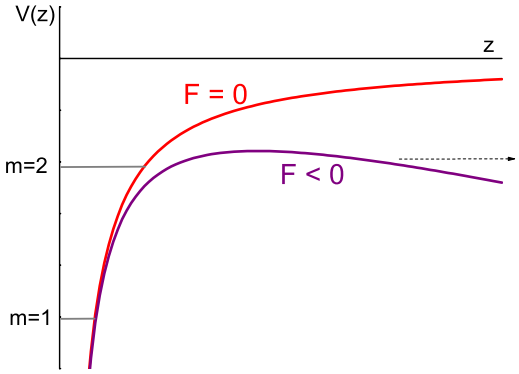

Figure 8. The potential with an extracting field. The arrow represents a tunneling electron.

7. Relaxation mechanisms

Relaxation mechanisms can be classified into two groups: Decay of the excited state (decoherence) and dephasing. In the decay of the excited state an electron makes a transition from state $|1\rangle$ to state $|0\rangle$. Decay leads to a finite lifetime T_1 of the excited state. Dephasing is the decay of the phase difference between the states $|0\rangle$ and $|1\rangle$. It leads to a finite phase coherence time T_2.

7.1. Decay of the excited state

Scattering of an electron off the helium surface waves involves absorption or emission of ripplons. During the decay process energy is absorbed by the in-plane vibrational states and momentum is absorbed by ripplons. Coupling of electrons to ripplons is weak. The ripplon amplitude δ_T is small compared to the average distance $\langle z \rangle$ of an electron from the surface,

$$\delta_T / \langle z \rangle \sim 2 \times 10^{-3} \text{ for } T = 10 \text{ mK}. \tag{22}$$

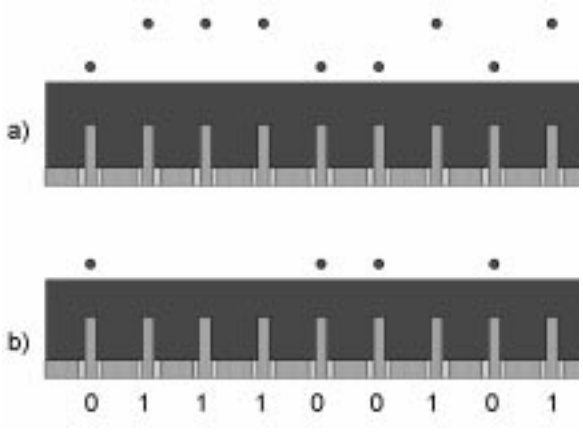

Figure 9. a) A nsec-ramp extracting field applied to the top plate extracts all electrons in the $|1\rangle$ state. b) Remaining electrons are in the $|0\rangle$ state and are detected by a superconducting bolometer (not shown in the figure) above the electrodes. The figure is not to scale.

Collin *et. al.*[10] measured the electron-ripplon scattering rate as ~ 2 MHz at $T = 300$ mK. Decay due to one-ripplon scattering is exponentially suppressed because the ripplons are very slow,

$$\omega_{\parallel} \gg \omega_r(q) \;\text{ for }\; q < (m\omega_{\parallel}/\hbar)^{1/2}. \tag{23}$$

Two-ripplon scattering can still cause decay. This is shown in Fig. 10. Momentum of electron is absorbed by two ripplons with wave vectors $\mathbf{q}_1$ and $\mathbf{q}_2 \approx -\mathbf{q}_1$. The energy is then absorbed by the vibrational states. The decay rate Γ^{2r} due to two-ripplon scattering is $< 4 \times 10^3$ s^{-1} corresponding to $T_1^{2r} > 250$ μs. Another

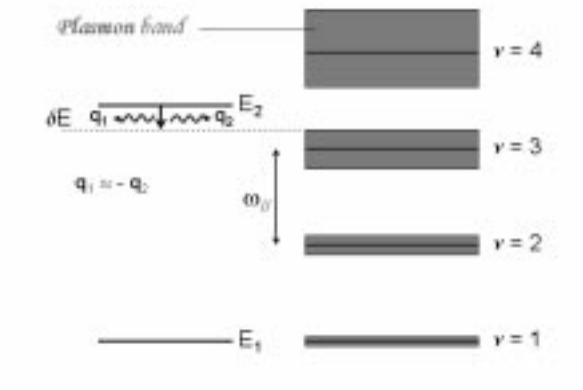

Figure 10. Two-ripplon decay process. Momentum of electron is absorbed by two ripplons with nearly equal momenta going nearly in opposite directions.

mechanism, phonon assisted decay of the excited state, causes a modulation of the helium surface. Phonons in the liquid also cause a modulation of the dielectric constant via a change in the helium density. The dominant decay mechanism is the spontaneous emission of a phonon in the bulk liquid and an excitation of the highest harmonic energy level that is beneath the energy of the excited state. The coupling to phonons through the phonon-induced modulation of the image potential gives $\Gamma^{ph} < 10^4$ s^{-1}, $T_2^{ph} > 100$ μs.

7.2. Dephasing

Dephasing results from the uncertainty of the energy due to scattering. The phase of the qubit states advances as,

$$\psi(t) \approx e^{i[U+eV(t)]t/\hbar}. \tag{24}$$

where $V(t)$ is the potential on the micro electrode. The energy U of the state is uncertain during a scattering process. Since the scattering amplitudes are different in states $|0\rangle$ and $|1\rangle$, the change in the energies of these states will differ. This can also be thought of as the modulation of the distance between the energy levels E_1 and E_2. The two-ripplon process for electrons confined to posts leads[8], at 10 mK, to $\Gamma_{\varphi}^{2r} \propto T^3 \sim 10^2$ s^{-1}, $T_2^{2r} \sim 10$ ms.

The dominant process is Johnson noise on the electrodes. The normal applied field can be estimated by treating the micro-electrode as a sphere with the diameter of the post. A voltage of 100 mV gives a field of ~ 200 V/cm for $h = 1$ μm. Such an applied voltage would tolerate a 25 Ω resistor heat sunk at 1 K. The Johnson noise for these parameters yields $\Gamma_{\varphi}^{el} < 10^4$ s^{-1}, $T_2^{2r} > 100$ μs.

In summary, the decay T_1 and dephasing T_2 times for a quantum computer based on electrons on helium are

$$T_1 \sim 100\ \mu\text{s}\ \ , T_2 \sim 100\ \mu\text{s}. \tag{25}$$

Single operations can occur in ≤ 10 ns. Thus 10^4 serial operations can be performed in a decoherence time. A computer made of electrons on liquid helium can, in principle, be scaled to an arbitrary number of qubits.

8. Technical difficulties

In a realistic quantum computer based on electrons on helium a number of obstacles must be overcome. The Stark fields are difficult to control precisely. The field is similar to that of a field emission tip,

$$V_{post} = 1\ \mu\text{V} \Rightarrow E = 1\ \text{mV/cm} \Rightarrow \Delta\nu = 1\ \text{MHz}. \tag{26}$$

The posts are probably non-uniform. Starks shifts will have to be experimentally calibrated for each post. Phase shifts due to electrostatic potentials must be taken into account. Voltages on posts influence neighboring electrons. Although interactions between qubits can be controlled, they can not be turned off. Implementation of a CNOT gate is difficult due to interaction with neighboring qubits when there are more than two qubits.

9. Results and Conclusions

We described a quantum computer based on electrons floating on liquid helium. Each qubit is made of combinations of ground and first excited states of an electron trapped laterally over micro-electrodes just below the helium surface. The technical difficulties are no more challenging than those of other proposed systems for quantum computation. We describe mechanisms for preparing the initial state of the qubit, operations with the qubits, and a proposed simultaneous readout scheme. The advantage of this system over other proposed systems is the simultaneous readout and the scalability. This system is capable of 10^4 serial operations in a decoherence time of ~ 100 μs.

Acknowledgements

The author wishes to acknowledge Arnold. J. Dahm and Mark I. Dykman for helpful conversations. This work was supported in part by NSF grant EIS 0085922.

References

[1] A review of concepts for quantum computers is given in *Fortschritte der Physik*, **48**, (2000), issues 9-11.

[2] P.M. Platzman and M.I. Dykman, *Science*, **284**, (1999), 1967.

[3] M.I. Dykman and P.M. Platzman, *Fortschr. Phy.*, **48**, (2000), 1095.

[4] A.J. Dahm, J.M Goodkind, I. Karakurt, S. Pilla, *J. Low Temp. Phys.*, **126**, (2002), 709.

[5] M.J. Lea, P.G. Frayne, and Yu. Mukharshy, *Fortschr. Phy.*, **48**, (2000), 1109.

[6] A.J. Dahm, J.A. Heilman, I. Karakurt, T. Peshek, *Physica E*, **18**, (2003), 169.

[7] C.C. Grimes and T.R Brown, *Phys. Rev. Lett.*, **32**, (1974), 280.

[8] M.I. Dykman, P.M. Platzman, P. Seddighrad, *Phys. Rev. B.*, **67**, (2002), 155402.

[9] G.F. Saville and J.M. Goodkind, *Phys. Rev. A.*, **50**, (1994), 2059.

[10] E. Collin, W. Bailey, P. Fozooni, P. Glasson, K. Harrabi, M.J. Lea, G. Papageorgiou *Phys. Rev. Lett.*, **89**, (2002), 245301.